TELKOMNIKA Indonesian Journal of Electrical Engineering
Vol.12, No.3, March 2014, pp. 2414 ~ 2421
DOI: http://dx.doi.org/10.11591/telkomnika.v12i3.4026

Electric Vehicle Lithium Ion Batteries Thermal Management

Gaoussou Hadia Fofana*, Youtong Zhang
Low Emission Vehicle Research Lab, Beijing Institute of Technology,
LABO Thermique Appliquée, ENI-ABT BAMAKO-MALI BP 242,
No. 5, Zhongguancun South Street, Haidian District, Beijing 100081, P. R. China
*Corresponding author, e-mail: fofanamali@yahoo.fr

Abstract

The lithium ion batteries, thanks to their high densities and high power, became promotes element for hybrid-electric and plug-in electric vehicles. Thermal management of lithium ion battery is important for many reasons, including thermal runaway, performance and maintains a constant temperature during the operating, security, lifecycle. However, in a battery pack, the batteries are stacked against each other without cooling surfaces except the outer surface of the package and the cell in the center of pack are exposed to overheating and thermal runaway. After several recent researches, it has been proved that lithium ion batteries are currently confronts a problem of temperature rise during their operation discharge, which affects the batteries performance, efficiency and reduces the life of lithium ion batteries. However, this work is set to access the three dimensional analytical modeling based on Green's Function technique to study the thermal behavior of lithium ion battery during discharge with different discharge rates (0.3C, C/2, 1C, 2C) and strategies natural convection cooling on the surface of the battery is performed.

Keywords*: lithium ion batteries, thermal management, 3D modeling, green's function, analysis*

1. Introduction

The lithium ion batteries are well known for their high densities of energy (*100-150Wh/kg*) and high power, with a large voltage (*3.8-4V*) and discharge rate, long cycle life, almost no memory effect and low self-discharge rate of approximately *5%* [1]. Currently, the electrification of the vehicle with lithium ion batteries to reduce the pollution of the atmosphere and the price of fuel is urgent. Lithium ion batteries became the favorable candidate because of its system of energy storage [2].

Several articles deal with the thermal models of batteries, which use different approaches such as: solving partial differential equations (PDE) [3], linear parameter-varying (LPV) models, the finite element models or lumped models. To enable an accurate simulation of the battery changes according to different temperature profiles used, or integrations, it is necessary to couple a thermal model and an electrochemical model, which are strongly dependent on one of the other. It is then possible to anticipate potential thermal runaway, designing appropriate systems of cooling and allow more efficient energy management [4, 5], However, for real-time implementation in a battery thermal management system (BTMS), some approaches, such as finite element modeling cannot be used because they are too costly in calculation. However, the challenge was reading on the application of lithium ion batteries on the hybrid vehicles and electric vehicles, which is controlling the temperature of the battery during operation by using lithium battery monitoring and control system [6]. Temperature rise occurs generally in the discharge of the batteries by electrochemical reactions (exothermic and the joule effect), which can cause thermal runaway, swelling of the battery and even the explosion in the most extreme cases. thermal management simulation is used to predicate the battery temperature during its operation condition (charge-discharge) and the modeling can determine the temperature distribution inside of batteries module during charge and discharge because several cell are connected together without enough cooling space.

Compared to recent study, the Green's Function and strategies natural convection cooling on the surface of the battery was used to investigate the heat generation of lithium ion

Received July 28, 2013; Revised October 10, 2013; Accepted October 31, 2013

batteries. The BTMSs are effective and the batteries are not critical but compulsory for safety, performance and long lifetime. It is necessary to maintain the temperature of the batteries in an ideal temperature range of *20~40*℃ and uniform the variations of temperature [7].

2. Research Method

The three-dimensional rectangular orthotropic solid of length L_1, width L_2, and Height L_3 was studied. Heat is generated within the solid domain, while heat transfer with surrounding medium is allowed at its boundary surfaces. The temperature distribution inside of batteries is described by energy balance equation that only includes conduction terms,

$$\rho c_p \frac{\partial T}{\partial t} = k_1 \frac{\partial^2 T}{\partial x^2} + k_2 \frac{\partial^2 T}{\partial x^2} + k_3 \frac{\partial^2 T}{\partial x^2} + g \tag{1}$$

Where ρ is density, c_p is heat capacity per unit mass, k_1 k_2 k_3 are the orthotropic thermal conductivity coefficients, $x=(x_1,x_2,x_3)$ represent the components of position vector in Cartesian coordinate system, t is time. The functions $T(x,t)$ and $g(x,t)$ represent the temperature filed and heat generation rate per unit volume.

The boundaries of the domain convective heat transfer are following [8, 9].

$$-k_i \frac{\partial T}{\partial x_i} + h_{i0}(T - T_0) = 0 \quad at \quad x_i = 0 \tag{2-1}$$

$$k_i \frac{\partial T}{\partial x_i} + h_{i0}(T - T_0) = 0 \quad at \quad x_i = L_i \tag{2-2}$$

The initial temperature of the domain (battery), T_0 is the ambient temperature, $T=T_0$ at $t=0$.

Let $X_i = \frac{x_i}{\sqrt{k_i}} (i = 1,2,3)$, $\theta = T - T_0$, $\tau = \frac{t}{\rho c_p}$, then:

$$\frac{\partial \theta}{\partial \tau} = \frac{\partial^2 \theta}{\partial X_1^2} + \frac{\partial^2 \theta}{\partial X_2^2} + \frac{\partial^2 \theta}{\partial X_3^2} + g \tag{3}$$

Boundary condition:

$$-\frac{L_i}{\sqrt{k_i}} \frac{\partial \theta}{\partial X_i} + Bi_{i0}\theta = 0 \quad at \quad X_i = 0 \tag{4-1}$$

$$\frac{L_i}{\sqrt{k_i}} \frac{\partial \theta}{\partial X_i} + Bi_{i1}\theta = 0 \quad at \quad X_i = \frac{L_i}{\sqrt{k_i}} \tag{4-2}$$

$Bi_{ij} = \frac{h_{ij} L_i}{k_i}$ are the Biot numbers.

And initial condition:

$\theta = T_o \quad at \quad \tau = 0$, where T_0 is the relevant temperature of 20℃. The temperature rise θ and the source for temperature rise G in temperature unit are $\theta = T_0$ [3], and;

$$G = \frac{g}{k_1 / L_1^2} \tag{5}$$

To determine the appropriate Green's function, we consider the homogeneous version of this problem as:

$$\frac{\partial^2\psi}{\partial x^2}+\frac{\partial^2\psi}{\partial y^2}+\frac{\partial^2\psi}{\partial z^2}=\frac{\partial\psi}{\partial t}\quad in\quad 0<x<a,0<y<b,0<z<c,t>0 \tag{6}$$

$$-\frac{L_i}{\sqrt{k_i}}\frac{\partial\psi}{\partial X_i}+Bi_{i0}\psi=0\quad at\quad X_i=0 \tag{7-1}$$

$$\frac{L_i}{\sqrt{k_i}}\frac{\partial\psi}{\partial X_i}+Bi_{i1}\psi=0\quad at\quad X_i=\frac{L_i}{\sqrt{k_i}} \tag{7-2}$$

$$a=\frac{L_1}{\sqrt{k_1}},\quad b=\frac{L_2}{\sqrt{k_2}},\quad c=\frac{L_3}{\sqrt{k_3}} \tag{8}$$

The desired Green's function is:

$$G(x,y,z,t\mid x',y',z',\tau)=\sum_{m=1}^{\infty}\sum_{n=1}^{\infty}\sum_{p=1}^{\infty}e^{-(\beta_m^2+\gamma_n^2+\eta_p^2)(t-\tau)}\frac{1}{N(\beta_m)N(\gamma_n)N(\eta_p)} \cdot X(\beta_m,x)X(\beta_m,x')Y(\gamma_n,x)Y(\gamma_n,y')Z(\eta_p,z)Z(\eta_p,z') \tag{9}$$

Then the solution of the three-dimensional transient, nonhomogeneous heat conduction problem $\theta(X_1,X_2,X_3,\tau)$ is:

$$\begin{aligned}\theta(X_1,X_2,X_3,T)&=\int_0^T g\,\mathrm{d}\tau\int_0^a\int_0^b\int_0^c G(X_1,X_2,X_3,T_1\mid X_1',X_2',X_3',\tau)\,\mathrm{d}X_1'\mathrm{d}X_2'\mathrm{d}X_3'\\&=\int_0^T g\,\mathrm{d}\tau\sum_{m=1}^{\infty}\sum_{n=1}^{\infty}\sum_{p=1}^{\infty}e^{-(\beta_m^2+\gamma_n^2+\eta_p^2)(t-\tau)}\frac{1}{N(\beta_m)N(\gamma_n)N(\eta_p)}X(\beta_m,x)Y(\gamma_n,x)Z(\eta_p,z)\int_0^a\int_0^b\int_0^c X(\beta_m,x')Y(\gamma_n,y')Z(\eta_p,z')\,\mathrm{d}X_1'\mathrm{d}X_2'\mathrm{d}X_3'\end{aligned} \tag{10}$$

As for integral,

$$\begin{aligned}&\int_0^a\int_0^b\int_0^c X(\beta_m,x')Y(\gamma_n,y')Z(\eta_p,z')\,\mathrm{d}X_1'\mathrm{d}X_2'\mathrm{d}X_3'\\&=\left(\int_0^a X(\beta_m,x')\,\mathrm{d}x'\right)\left(\int_0^a Y(\gamma_n,y')\,\mathrm{d}y'\right)\left(\int_0^a Z(\eta_p,z')\,\mathrm{d}z'\right)\\&=\left(\sin\beta_m a-\frac{H_{11}}{\beta_m}\cos\beta_m a+\frac{H_{11}}{\beta_m}\right)\left(\sin\gamma_n b-\frac{H_{21}}{\gamma_n}\cos\gamma_n b+\frac{H_{21}}{\gamma_n}\right)\left(\sin\eta_p c-\frac{H_{31}}{\eta_p}\cos\eta_p c+\frac{H_{31}}{\eta_p}\right)\end{aligned} \tag{11}$$

So,

$$\theta(X_1,X_2,X_3,\tau)=\frac{g}{N(\beta_m)N(\gamma_n)N(\eta_p)}X(\beta_m,x)Y(\gamma_n,x)Z(\eta_p,z)\frac{1}{\beta_m^2+\gamma_n^2+\eta_p^2}\left(1-e^{-\left(\beta_m^2+\gamma_n^2+\eta_p^2\right)\tau}\right) \tag{12}$$

This paper used a simple lithium ion battery examined to analysis thermal management of Lithium ion batteries. Figure 1 shows prismatic Lithium ion cells used in the battery for hybrid-electric and plug-in electric vehicles (H/PEVs) applications. As for the thermal parameters of lithium ion battery, the thickness and thermophysical properties of the battery core layers and materials are provided in literature. Thickness, number of layers, density, heat capacity, and thermal conductivity values are provided. Porous polymer layers must be measured after they are soaked in the electrolyte liquid in the electrodes and separator sheets. Meanwhile heat

capacity and thermal conductivity of wet layers use available data in the literature for a similar battery type.

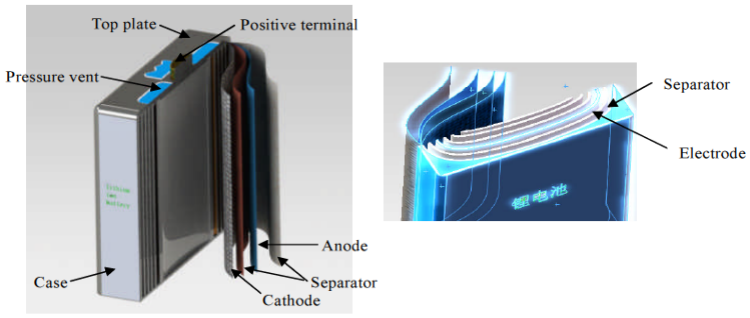

(a) (b)

Figure 1. (a) Multi-folded-layer structure of a prismatic cell; (b) Sectional view of X-ray pictures showing battery layers in the cell

Based on Figure 1, for polymer lithium ion batteries, since the contact interfaces are wet at the presence of the electrolyte liquid, the effects of contact resistance are assumed to be negligible. This simplification is usually justified with the fact that thermal conductivities of electrolyte and polymer compounds are in the same order. Detailed experimental study on contact resistance issue in batteries is not available, and the authors believe that this important phenomenon is overlooked and plan to further investigate this potentially critical issue in depth. Due to its small thickness and polyethylene laminates, the heat capacity and thermal conductivity of the case is negligible, hence, its effects can be excluded from the thermal analysis. In order to complete the initial boundary value problem in (3) and (4), heat generation rate *g(x,t)* should be determined. One of the most challenging tasks in thermal modeling of batteries is the evaluation of heat generation rate during their operation. Complexities associated with this task are rooted in the strong coupling of heat generation rate to chemical reactions rates, and Joule heating inside the battery structure [10].

Bernardi proposed a general energy balance equation [3] for battery thermal models in which the homogeneous heat generation rate is given by:

$$g = \frac{I}{\upsilon}\left[\left(V_{oc} - V\right) - T\frac{dV_{oc}}{dT}\right] \quad (13)$$

The above formula simulates detailed thermal analysis. *v* is the volume of the battery, V_{oc} is open circuit potential, *V* and *I* is the voltage and current of the battery. For lithium ion batteries, during normal operational temperatures, the derivative dV_{oc}/dT is a very small constant [7] and can be safely neglected [11] Keeping intense attention that, V_{oc} is a strong function of ion concentration, and not the temperature in lithium ion batteries, which is measured in non-operating condition, Nonetheless, at very high and low temperatures the dependency of V_{oc} on temperature is considerable [12].

Experimental data, reported by lithium ion batteries, on variation of cell potential (voltage) versus depth of discharge (DOD) for different discharge rates are shown in Figure 2. For discharge processes, the cut-off voltage of *2.8 V* is considered.

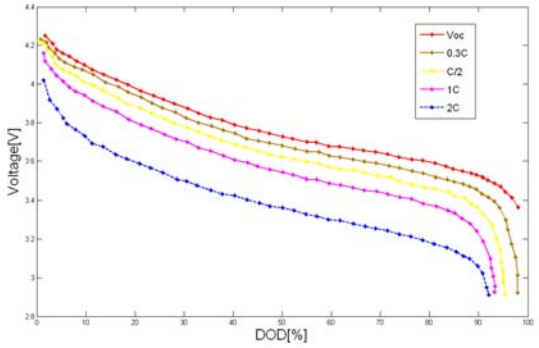

Figure 2. The Experimental Data on Variation of Battery Voltage Versus DOD for Different Discharge Conditions in C-rate

3. Results and Discussion

As for different discharge modes, homogeneous heat generation rates *g=g(t)*, are obtained by fitting high-order polynomials to the data points in Figure 2, and using $dV_{oc}/dT \approx 0$ [13] Curves in Figure 3 show the variation of volumetric heat generation rates versus DOD during discharge processes (*C/2, 1C, 2C*). The sharp increase of g at the end of discharge is rooted in the large differences between V_{oc} and operating voltages.

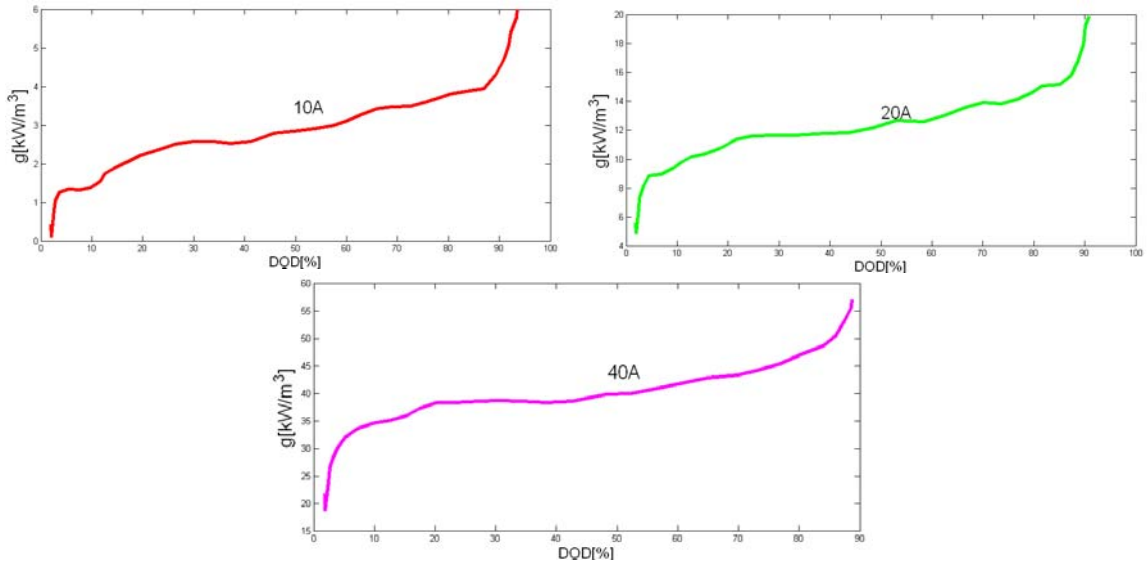

Figure 3. Variation of Heat Generation Rate Versus DOD during Discharge Processes (C/2, 1C, 2C) Experimental Data

Battery thermal management systems run procedure based on heat transfer at battery surfaces depended on different parameters, this paper assumes small and moderate heat transfer coefficients *h <20*, cooling with air. *h* at all surfaces are considered as constant, albeit the method can handle different values for heat transfer coefficients. The ambient and initial temperature is T_0*=20* ℃, thus, based on the recommended operation temperature (*-30 ~50* ℃), the maximum temperature rise of $\theta = \Delta T = T - T_0 = 30℃$ is acceptable during the battery operation. Throughout the results, this trend of the minimum temperature is more visible in Figure 4, which indicates temperatures rise, is closed relative to the convective heat transfer coefficients *h*, alone with DOD, *h* becomes bigger, θ will becomes smaller.

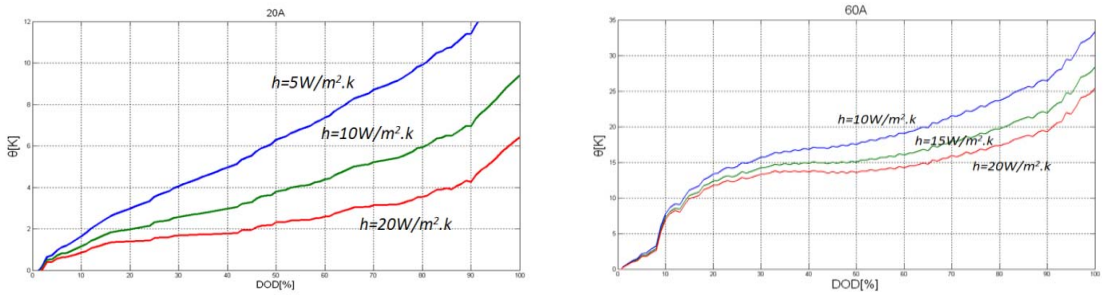

(a) (b)

Figure 4. (a) Temperature Rise in the Battery during *20A* Discharge (*h=5, 10, 20W/m²-K*); (b) Temperature rise in the Battery during *60A* Discharge (*h=10, 15, 20 W/m²-K*)

The temperature distribution at the end of a *40A* and *60A* discharge process is shown in Figure 5 and Figure 6.

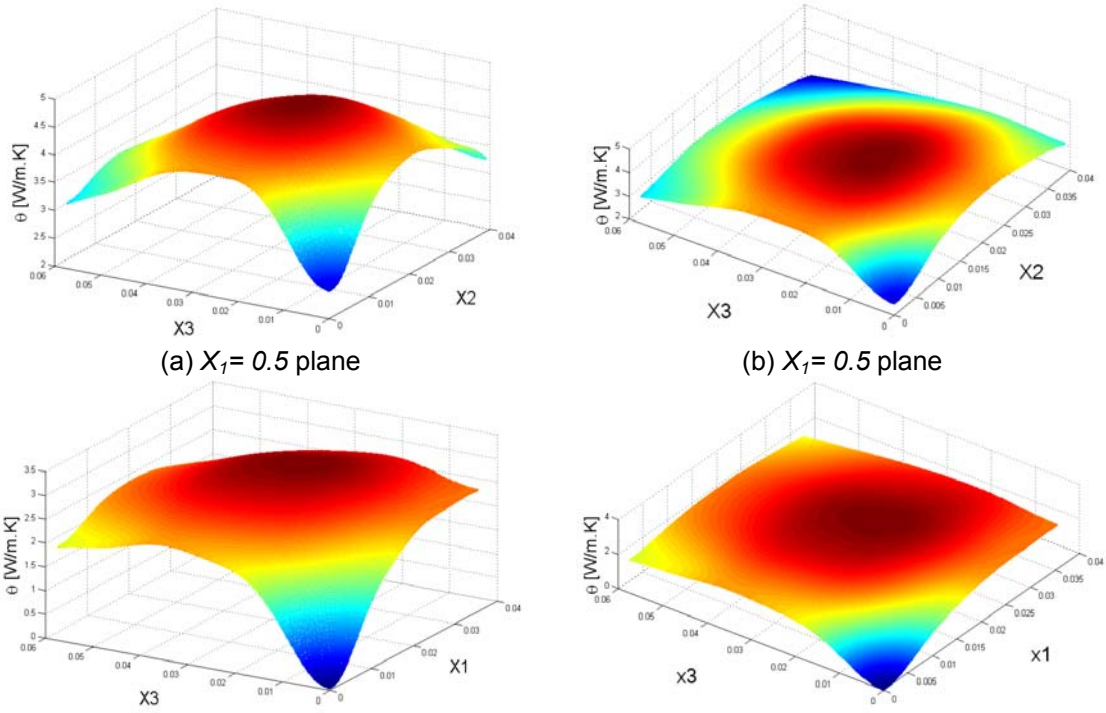

(a) X_1= *0.5* plane (b) X_1= *0.5* plane

(c) X_2= *0.5* plane (d) X_2= *0.5* plane

Figure 5. Temperature Rise at *40A* Discharge with *h = 25 W/m²-K*

Plots (a)-(d) in Figure 5 have the maximum temperature rise of $\theta_{\max}$ =*6.9K*, the best geometry choice for a two-dimensional modeling is x_3-x_2 section surface. Figure 5 shows temperature rise at the end of a *40 A* discharge process is on X_1=*0.5*, X_2=*0.5* section. Maximum temperature rise $\theta_{\max}$ at the center of the battery, and minimum temperature rise $\theta_{\min}$ at the corners of the battery, e.g., since Biot number in x_2 -direction is always less than the other two directions, a two-dimensional model in x_1-x_3 plane is also acceptable. Note that increasing of *h* in x_2 -direction can change the choice for a two-dimensional model.

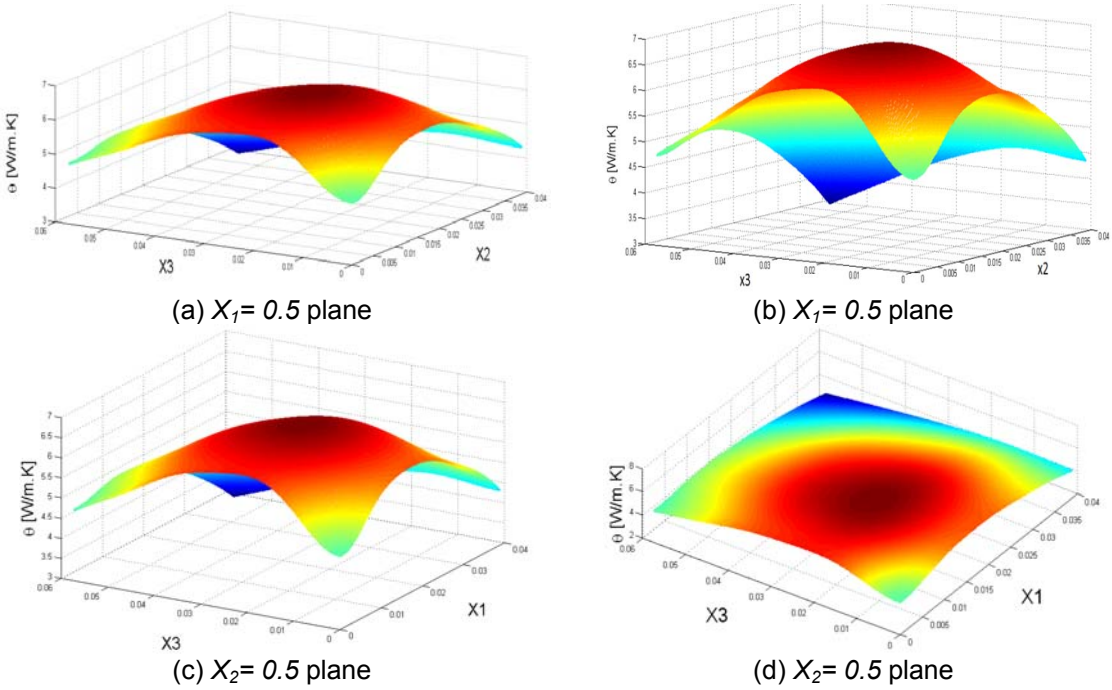

(a) X_1= *0.5* plane (b) X_1= *0.5* plane

(c) X_2= *0.5* plane (d) X_2= *0.5* plane

Figure 6. Temperature Rise at *60A* Discharge with *h = 25 W/m*^{2}*-K*

In Figure 6, temperature rise distribution at the end of a *60A* discharge process with the above non-homogeneous heat generation rate is shown on X_1= *0.5*, X_2= *0.5* planes. Boundary conditions at all surfaces are the same with *h = 25W/m*^{2}*-K*. As $X_3 \rightarrow 1$, the magnitude of joule heating increases and in contrast to the case of homogeneous heat generation, location of $\theta_{\max}$ is not at the battery center but near the positive tab.

By using the Green's Function and strategies natural convection cooling on the surface of the battery, we can deeply investigate the heat generation of lithium ion batteries.

4. Conclusion

In this paper, the classical mechanism analysis technique of Green's function was used to control the temperature distribution of lithium ion batteries during discharge process; a closed-form solution was proposed to study the temperature distribution in simple battery model. The proposed approach takes account for, thermal conductivities, Multi-dimensional heat diffusion, convective boundary condition, transient heat generation rate. And it provided a useful and reliable approach for investigating thermal behavior of batteries under various conditions. The proposed analytical model was employed to study the temperature distribution in a single prismatic lithium ion battery during discharge processes, where transient heat generation rate was approximated from the electrical performance of the battery. In large battery assemblies the issue of temperature rise becomes more and more critical, as heat accumulates at the center of the battery module.

References

[1] Iezhou Wu, Lunan Liu, Qing Xiao, et al. Research on SOC estimation based on second-order RC model. *TELKOMNIKA Indonesian Journal of Electrical Engineering*. 2012; 10(7): 1667-1672.
[2] Ma Rong Jun. Progress of Research and Application on Negative Electrode Material for Lithium Ion Battery. *Nonferrous Metals*. 2008; 60(2): 38-45.
[3] D Bernardi, E Pawlikowski, J Newman. A General Energy Balance for Battery Systems. *Electrochem. Soc.*, 1985; 132(1): 5-12.
[4] Guo Bing Kun, Xu Hui, Wang Xian you. Lithium ion battery. Changsha: Central south university press. 2002.

[5] Cheng Xi Ming, Sun Feng Chun. Overview of energy storage technology for Electric Vehicles. *Chinese Journal of Power Sources*. 2001; 25(1): 47-52.
[6] Lei Lin, Yuankai Liu, Wang Ping, Fang Hong. The Electric Vehicle Lithium Battery Monitoring System. *TELKOMNIKA Indonesian Journal of Electrical Engineering*. 2013; 11(4): 2247-2252.
[7] P Taheri, M Bahrami. Temperature Rise in Prismatic Polymer Lithium-Ion Batteries: An Analytic Approach. *SAE Int. J. Passeng. Cars - Electron. Electr. Syst.*, 2012; 5(1): 164-176.
[8] Özişik MN. Heat Conduction. 2nd ed., New York: John Wiley & Sons. 1993.
[9] Thapa AK, Park G, Nakamura H, Ishihara T, Moriyama N, Kawamura T, Wang H, Yoshio M. Novel graphite/TiO2 electrochemical cells as a safe electric energy storage system. *Electrochimica Acta.* 2010; 55(24): 7305-7309.
[10] KM Abraham, SB Brummer. *J. P. Gabano, Editor*. Lithium Batteries. New York: Academic Press. 1983.
[11] GL Plett. Extended Kalman filtering for battery management systems of LiPB-based HEV battery packs: Part 1. Background. *Power Sources*. 2004; 134(2): 252-261.
[12] Hu Y, Yurkovich S, Guezennec Y, Yurkovich BJ. Electro- thermal battery model identification for automotive applications. *Power Sources*. 2011; 196(1): 449–457.
[13] HS Carslaw, JC Jaeger. Conduction of Heat in Solids. 2nd Ed. Oxford: Clarendon Press. 1959.